

Internuclear Separation Dependent Ionization of the Valence Orbitals of I₂ by Strong Laser Fields

H. Chen, V. Tagliamonti, and G. N. Gibson

Department of Physics, University of Connecticut, Storrs, Connecticut 06269, USA

(Received 21 May 2012; published 8 November 2012)

Using a pump-dump-probe technique and Fourier-transform spectroscopy, we study the internuclear separation R dependence and relative strength of the ionization rates of the π and σ electrons of I₂, whose valence orbitals are $\sigma_g^2 \pi_u^4 \pi_g^4 \sigma_u^0$. We find that ionization of the highest occupied molecular orbital (HOMO)-2 (σ_g) has a strong dependence on R while the HOMO and HOMO-1 do not. Surprisingly, the ionization rate of the HOMO-2 exceeds the combined ionization rate of the less bound orbitals and this branching ratio increases with R . Since our technique produces target molecules that are highly aligned with the laser polarization, the σ orbitals will be preferentially ionized and undergo enhanced ionization at larger R compared to the π orbitals. Nevertheless, it is highly unusual that an inner orbital provides the dominant strong field ionization pathway in a small molecule.

DOI: [10.1103/PhysRevLett.109.193002](https://doi.org/10.1103/PhysRevLett.109.193002)

PACS numbers: 33.80.Rv, 32.80.Rm, 42.50.Hz

Exposing molecules to strong laser fields produces a variety of effects, which has led to considerable work in many areas, such as high harmonic generation [1–4], non-sequential double ionization [5,6], and coherent control [7,8]. In virtually all of these phenomena, single-electron ionization of the neutral ground state molecule is the critical first step. However, single-electron ionization is still not well-understood, given the many degrees of freedom in a molecule (rotational, vibrational, and electronic).

In particular, the ionization rate as a function of internuclear separation R , $\Gamma(R)$, has become a topic of much research, leading to the phenomena of Enhanced Ionization (EI) [9–14] in which $\Gamma(R)$ peaks at a certain critical separation R_c , and Lochfrass [15–18] in which a vibrational wave packet (VWP) in the ground electronic state (GES) of neutral molecules is formed due to a large slope of $\Gamma(R)$ at the equilibrium separation R_e . However, the VWP generated through Lochfrass only vibrates within a very small range of R around R_e , prohibiting extended measurements of $\Gamma(R)$. For I₂, there is even disagreement between the experimental results and the theoretical predictions on whether the slope of $\Gamma(R)$ is positive or negative at R_e . The experiment implies $d\Gamma/dR > 0$ at R_e [17], while the dependence of ionization potential on R implies just the opposite [19–21]. To fully understand $\Gamma(R)$ of the GES, a VWP vibrating over a large range of R is needed.

While most experiments consider ionization from the highest occupied molecular orbital (HOMO), it has been known for some time that inner-orbital ionization occurs in strong laser fields [22]. Recently, ionization from inner orbitals is attracting more attention [3,23,24]. However, for small light-atom molecules, like N₂, O₂, CO₂, and HCl, the ionization branching ratio of inner orbitals is usually rather small, given the large differences in ionization potentials, compared with the HOMO. To better understand the role of inner-orbital ionization in strong fields, these studies must be extended to both large light-atom

molecules, like uracil [25], and small heavy-atom molecules, like I₂.

To study the ionization of a ground state neutral molecule, we use a pump-dump-probe scheme to create a coherent VWP in the GES of I₂, whose valence orbitals are $\sigma_g^2 \pi_u^4 \pi_g^4 \sigma_u^0$. The VWP vibrates between 4.4 and 6.2 a.u., over which $\Gamma(R)$ is measured. The single ionization from different orbitals is determined from analyzing the final states and Fourier-transform spectroscopy. We will show that $\Gamma(R)$ actually increases with R , consistent with the experimental results of Lochfrass. However, the increased ionization comes from the HOMO-2 (σ_g), but not from the HOMO (π_g) or HOMO-1 (π_u). In fact, the ionization rate of the HOMO-2 exceeds that of the combined rate of the less bound orbitals and this branching ratio increases with R . To our knowledge, this has never been seen in small light-atom molecules.

The pump-dump-probe scheme is shown in Fig. 1. The VWP is first launched to the B state of I₂ by a weak 525 nm pump pulse through a one-photon resonant transition, brought back to the GES by a weak 800 nm dump pulse through resonant deexcitation, and finally, singly ionized by a delay-controllable 800 nm probe pulse. All pulses are linearly polarized along the time-of-flight (TOF) axis, except where noted. Since the X - B transition is a parallel transition [26], the molecules excited to the B state will be aligned with the pump laser polarization with a $\cos^2(\theta)$ distribution [14], and the ones deexcited back to the X state will have a higher degree of alignment, $\cos^4(\theta)$.

The experiments are performed with one of two ultrafast Ti:sapphire laser systems (a homebuilt or a Spectra-Physics) and a TOPAS (optical parametric amplifier) system. The ionization signals of I₂⁺, I⁺, and I²⁺ are recorded with a TOF spectrometer. Room temperature (295 K) I₂ gas is leaked effusively into the chamber with a base pressure of 2×10^{-9} torr. The Ti:sapphire laser produces linearly polarized pulses (800 nm, 37 fs (homebuilt) or 50 fs

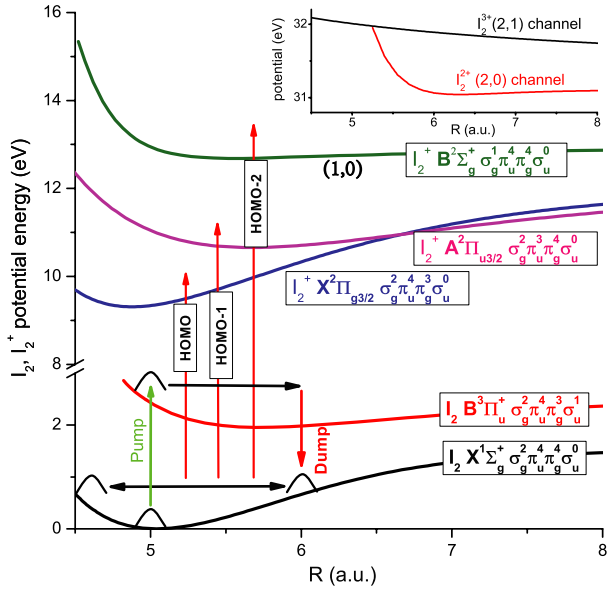


FIG. 1 (color online). Schematic potential energy curves, showing the physical scenario of the pump-dump-probe experiments.

(Spectra-Physics), 1 kHz, up to 800 μJ) and the output beam is split with $\sim 80\%$ of the energy sent into the TOPAS to generate a pump beam (525 nm, 50 fs, up to 2 μJ) while the rest is sent to another beam splitter to generate the dump and probe beams. An aperture is used in either of the first two beams in order to decrease ionization by the pump and dump pulses, while creating a more uniform focal volume for the probe pulse. The pump-dump delay τ_{p-d} , and the dump-probe delay τ_{d-pr} are adjusted by two computer controlled translational stages. From the separation of the peaks in the TOF spectrum, one can determine the momentum and kinetic energy release (KER) of a pair of dissociating fragments. More details can be found in Refs. [14,27].

To find the best τ_{p-d} , we fix the delay between the pump and probe pulses at 0.3 ps and scan the dump pulse. The depletion of the B state can be found by looking at the variation of the I_2^+ signal in the (2,1) channel [the (m,n) channel refers to the dissociating channel $I_2^{(m+n)+} \rightarrow I^{m+} + I^{n+}$] which results from ionizing the B state, as seen in Fig. 2(a). The maximum depletion is around 75% and occurs at $\tau_{p-d} = 0.045$ ps, as shown in Fig. 2(b), consistent with simulations.

We fix τ_{p-d} for maximum depletion and scan τ_{d-pr} to obtain the ionization signals of I_2^+ as a function of R to characterize the X -state VWP. In Fig. 3(a), we see the expected VWP motion in the (2,0) channel [27]. We further analyze the data by taking a Fourier transform of the delay variable τ_{d-pr} . The FFT of the signal in the (2,0) channel in Fig. 3(b) gives not only the frequency of the vibration, but also the KER of the VWP in the X state projected onto the (2,0) state. There are two frequencies, 6.3 THz at large

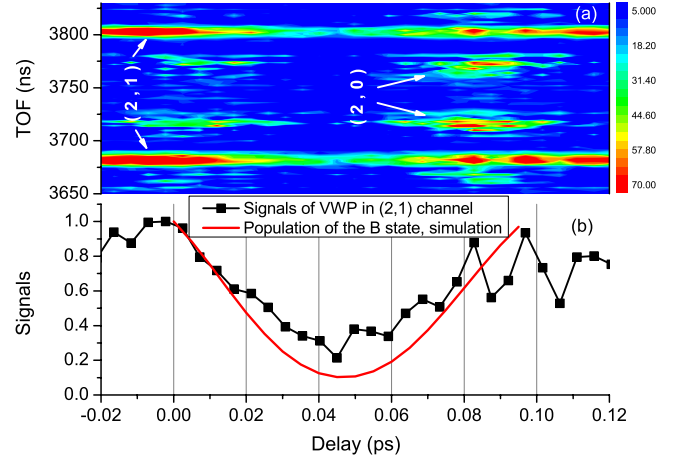


FIG. 2 (color online). (a) The TOF of I_2^+ as a function of τ_{p-d} (background subtracted) with a step size of 0.005 ps with the pump-probe delay fixed at 0.3 ps. (b) The depletion of the B state as a function of τ_{p-d} from the simulation (red line, normalized), and experiment (black line with data points, normalized). The experimental data correspond to the integrated signal in the range of 3670–3700 ns in (a). In the experiment, the intensities of the pump, dump, and probe pulses are estimated to be $\sim 1.2 \times 10^{11}$, $\sim 1.3 \times 10^{12}$, and $\sim 2.4 \times 10^{13}$ W/cm², respectively, and the I_2 pressure is $\sim 7.0 \times 10^{-7}$ torr.

KER associated with an R near R_e which is created through Lochfrass or bond-softening from the dump pulse (see below) [17], and 5 THz at lower KER associated with large R which corresponds to the returning VWP. The variation of the KER of the returning VWP in the (2,0) channel directly maps the motion of the VWP as a function of R , with the largest and smallest KER corresponding to the

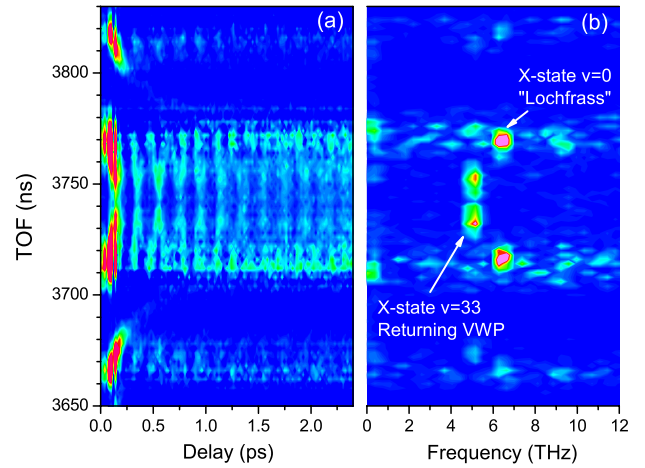


FIG. 3 (color online). (a) The TOF plot of the (2,0) and (2,1) channels as a function of τ_{d-pr} with a step size of 0.020 ps with τ_{p-d} fixed at 0.045 ps, showing the returning VWP in both of the two channels. The background has been subtracted, and the experimental parameters are the same as in Fig. 2. (b) The FFT plot of the delay variable of (a).

smallest and largest R , respectively. Simulations confirm the vibrational frequency of 5 THz, which corresponds to an average vibrational quantum number of 33 and a VWP motion between 4.4 and 6.2 a.u.

Since we see both the 5 and 6.3 THz modulations in the (2,0) channel, we expect to see them in the I_2^+ signal, as well, allowing us to measure $\Gamma(R)$ over a large range of R . If we found a strong 5 THz component in the FFT of the I_2^+ signal, its phase would give us a new measurement of the slope of $\Gamma(R)$. Surprisingly, the FFT shows no 5 THz modulation, but only a 6.3 THz modulation in the I_2^+ signal, as seen in Fig. 4(a). However, there is a strong 5 THz component in the (1,0) channel [Fig. 4(a)] which shows that the VWP is actually ionized to this dissociating channel. The ionization rate of the (1,0) channel is out of phase with the momentum of the VWP in the (2,0) channel [Fig. 4(b)], showing that $\Gamma(R)$ of the X state increases with R , in good agreement with our previous study of Lochfrass [17]. Moreover, from Fig. 3(a), we only see the VWP vibrating within the normal range of the (2,0) channel, showing that $\Gamma(R)$ at $R < R_e$ is vanishingly small. If not, we would see an abnormally high KER in the (2,0) channel associated with ionization at $R < R_e$.

In order to check that these results are from the excited X -state VWP and not residual population in the B state, we ran the experiment with the pump and probe pulses polarized as before, but a perpendicularly polarized dump pulse. Because the B state is aligned horizontally with the

pump pulse, the vertical dump pulse will not deplete it. As seen in Fig. 4(a), both the 5 and 6.3 THz modulation disappear, showing that the dump pulse, indeed, generates the 6.3 THz signal and the 5 THz signal does not come from the B -state VWP.

Having established that the 5 THz signal comes from the large amplitude VWP in the X state of I_2 , we need to understand why it occurs in the (1,0) and not the I_2^+ channel. Single ionization of the HOMO, HOMO-1, and HOMO-2 of I_2 will leave the molecule in the $X^2\Pi_{1/2,3/2g}$ ($\sigma_g^2\pi_u^4\pi_g^3\sigma_u^0$), $A^2\Pi_{1/2,3/2g}$ ($\sigma_g^2\pi_u^3\pi_g^4\sigma_u^0$), and $B^2\Sigma_g^+$ ($\sigma_g^1\pi_u^4\pi_g^4\sigma_u^0$) states of I_2^+ , respectively. These five states are clearly seen in extreme ultraviolet photoelectron spectroscopy [28]. The X and A states are bound and both contribute to the I_2^+ signal, while the B state dissociates, leading to the (1,0) channel [19,28]. Thus, ionization of the HOMO-2 will produce a (1,0) signal, although we must consider the other source of (1,0): resonant population transfer in the molecular ion.

As the molecule vibrates, electronic states will go in and out of resonance. At a resonance, population can be transferred from the bound X and A states to the dissociating B state and visa versa. Thus, the (1,0) channel could arise from a two-step process involving ionization of the HOMO or HOMO-1 and subsequent resonant excitation. Moreover, this process would be modulated at 5 THz. However, population transfer would simultaneously increase one signal while decreasing another, so both would be modulated at 5 THz with the same amplitude and opposite phase. As a 5 THz modulation is not seen in the I_2^+ signal, resonant population transfer in the molecular ion can be ruled out. Hence, the (1,0) channel must be associated with the B state of I_2^+ through single ionization of the HOMO-2 σ_g orbital.

Based on this assignment, we can write the single ionization rate of the GES of I_2 as $\Gamma_X(R) = \Gamma_{XX}(R) + \Gamma_{XA}(R) + \Gamma_{XB}(R)$, where $\Gamma_{XX}(R)$, $\Gamma_{XA}(R)$, and $\Gamma_{XB}(R)$ are the ionization rates of the HOMO π_g electron, HOMO-1 π_u electron, and HOMO-2 σ_g electron, respectively. The first two combined give the rate to I_2^+ , and the last one gives the rate to the (1,0) channel and since we find the 5 THz modulation in the (1,0) channel and not the I_2^+ , ionization of the HOMO and HOMO-1 does not have a strong dependence on R , while the ionization of the HOMO-2 does. We have previously seen that the ionization of the B state of I_2 also has a strong dependence on R [14]. We attributed this strong dependence to EI as the outer orbital in the B state is a σ_u and EI is expected for σ orbitals [12]. Similarly, the HOMO-2 is a σ_g and should also experience EI, giving rise to a strong modulation in our experiment. It is also predicted that π orbitals will not have EI [12] and, as a result, their ionization rate does not have nearly as strong a dependence on R —explaining the lack of modulation of our I_2^+ signal. Moreover, our pump-dump-probe technique produces target molecules

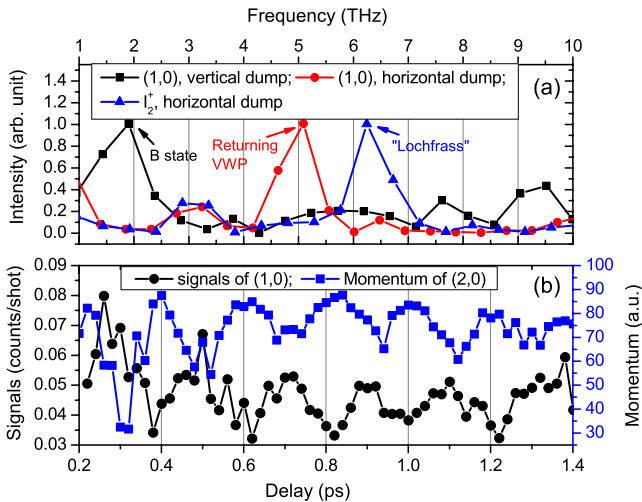


FIG. 4 (color online). (a) The FFT spectra of the (1,0) signal and the bound I_2^+ signal (normalized). The data were taken with a step size of 0.020 ps, and the FFT curves were obtained by integrating the forward going (1,0) signals or the whole I_2^+ signals and then performing an FFT. (b) Variation of the signal in the (1,0) channel and the momentum of the returning VWP in the (2,0) channel as a function of τ_{d-pr} . The intensities of the pump, dump, and probe pulses are estimated to be $\sim 7.5 \times 10^{11}$, $\sim 1.4 \times 10^{12}$, and $\sim 6.2 \times 10^{12}$ W/cm², respectively. The I_2 pressure is $\sim 7.2 \times 10^{-7}$ torr.

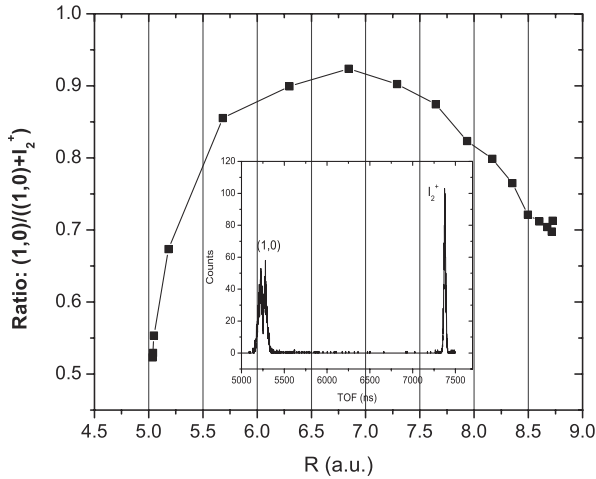


FIG. 5. The branching ratio of the (1,0) signal ionizing from the B state as a function of R [branching ratio: (1,0) signal divided by the whole ionization signal]. Inset: the TOF signal of the (1,0) and bound I_2^+ with a single 800-nm laser pulse with an intensity of $\sim 6.2 \times 10^{12}$ W/cm 2 , and the branching ratio of the (1,0) signal is 65.2%.

well aligned along the TOF axis providing the best comparison of EI in σ and π orbitals.

One final observation corroborates our conclusion that the observed R dependence of the ionization rate of the valence orbitals of I_2 is due to their σ or π character. In light molecules, such as N_2 , O_2 , or CO_2 , the contribution of the inner-orbitals is small compared to the HOMO as a result of their larger binding energies. However, in I_2 , we find that the single pulse branching ratio at R_e is 65% for ionization of the HOMO-2, as shown in the inset of Fig. 5, indicating that the orbital geometry is more important in determining the ionization rate than the relative ionization potential of the orbitals. In a related experiment [14], we determined this branching ratio as a function of R by launching a VWP on the B state of I_2 . We find that the branching ratio of the (1,0) channel increases with R , reaches a peak at around 6.85 a.u. and then drops again, as shown in Fig. 5. While this experiment uses the B state of I_2 ($\sigma_g^2 \pi_u^4 \pi_g^3 \sigma_u^1$) as the initial state, the ionization from the X state VWP will likely have the same property. Indeed, the branching ratio should be higher, because ionization to the bound I_2^+ state from the B state is easier than from the X state, with the former requiring the removal of one electron from the LUMO and the latter requiring ionization from the HOMO. For instance, the branching ratio of the (1,0) signal ionizing from the X state (65.2%) is higher than that from the B state (52.7%) at the same R of 5.03 a.u.. The increasing branching ratio as a function of R is consistent with the strong dependence of the ionization rate for σ orbitals and the weak dependence for π orbitals.

In conclusion, we generate a coherent VWP in the GES of neutral I_2 and the target molecules are highly aligned with the laser polarization. This is a new way to study the behavior of the GES of molecules in strong laser fields. The R dependence and relative strength of the ionization rates of different orbitals of I_2 have been discussed. The ionization rates of the HOMO (π_g) and HOMO-1 (π_u) initially increase with R but level off; however, the ionization rate of the HOMO-2 (σ_g) keeps increasing with R , presumably until R_c , where EI is reached. Finally, the HOMO-2 provides the dominant ionization pathway, which is highly unusual for strong field ionization.

We would like to acknowledge support from the NSF under Grant No. PHYS-0968799.

- [1] Z. Chang, A. Rundquist, H. Wang, M. M. Murnane, and H. C. Kapteyn, *Phys. Rev. Lett.* **79**, 2967 (1997).
- [2] J. Itatani, J. Levesque, D. Zeidler, H. Niikura, H. Pépin, J. C. Kieffer, P. B. Corkum, and D. M. Villeneuve, *Nature (London)* **432**, 867 (2004).
- [3] B. K. McFarland, J. P. Farrell, P. H. Bucksbaum, and M. Gühr, *Science* **322**, 1232 (2008).
- [4] E. Hijano, C. Serrat, G. N. Gibson, and J. Biegert, *Phys. Rev. A* **81**, 041401(R) (2010).
- [5] D. N. Fittinghoff, P. R. Bolton, B. Chang, and K. C. Kulander, *Phys. Rev. Lett.* **69**, 2642 (1992).
- [6] C. Guo, M. Li, J. P. Nibarger, and G. N. Gibson, *Phys. Rev. A* **61**, 033413 (2000).
- [7] C. Trallero-Herrero, D. Cardoza, T. C. Weinacht, and J. L. Cohen, *Phys. Rev. A* **71**, 013423 (2005).
- [8] C. Trallero-Herrero and T. C. Weinacht, *Phys. Rev. A* **75**, 063401 (2007).
- [9] T. Zuo and A. D. Bandrauk, *Phys. Rev. A* **52**, R2511 (1995).
- [10] T. Seideman, M. Yu. Ivanov, and P. B. Corkum, *Phys. Rev. Lett.* **75**, 2819 (1995).
- [11] E. Constant, H. Stapelfeldt, and P. B. Corkum, *Phys. Rev. Lett.* **76**, 4140 (1996).
- [12] G. L. Kamta and A. D. Bandrauk, *Phys. Rev. A* **75**, 041401(R) (2007).
- [13] G. N. Gibson, M. Li, C. Guo, and J. Neira, *Phys. Rev. Lett.* **79**, 2022 (1997).
- [14] H. Chen, L. Fang, V. Tagliamonti, and G. N. Gibson, *Phys. Rev. A* **84**, 043427 (2011).
- [15] E. Goll, G. Wunner, and A. Saenz, *Phys. Rev. Lett.* **97**, 103003 (2006).
- [16] Th. Ergler, B. Feuerstein, A. Rudenko, K. Zrost, C. D. Schröter, R. Moshhammer, and J. Ullrich, *Phys. Rev. Lett.* **97**, 103004 (2006).
- [17] L. Fang and G. N. Gibson, *Phys. Rev. Lett.* **100**, 103003 (2008).
- [18] L. Fang and G. N. Gibson, *Phys. Rev. A* **78**, 051402(R) (2008).
- [19] W. A. de Jong, L. Visscher, and W. C. Nieuwpoort, *J. Chem. Phys.* **107**, 9046 (1997).
- [20] Jianwei Che, J. L. Krause, M. Messina, K. R. Wilson, and Y. Yan, *J. Phys. Chem.* **99**, 14949 (1995).
- [21] A. Saenz, *J. Phys. B* **33**, 4365 (2000).

-
- [22] G.N. Gibson, R.R. Freeman, and T.J. McIlrath, *Phys. Rev. Lett.* **67**, 1230 (1991).
- [23] D. Pavicic, K.F. Lee, D.M. Rayner, P.B. Corkum, and D.M. Villeneuve, *Phys. Rev. Lett.* **98**, 243001 (2007); S. Petretti, Y. V. Vanne, A. Saenz, A. Castro, and P. Declava, *Phys. Rev. Lett.* **104**, 223001 (2010).
- [24] H. Akagi, T. Otobe, A. Staudte, A. Shiner, F. Turner, R. Dörner, D. M. Villeneuve, and P. B. Corkum, *Science* **325**, 1364 (2009).
- [25] M. Kotur, T. C. Weinacht, C. Zhou, and S. Matsika, *Phys. Rev. X* **1**, 021010 (2011).
- [26] H. Stapelfeldt, E. Constant, and P. B. Corkum, *Phys. Rev. Lett.* **74**, 3780 (1995).
- [27] L. Fang and G. N. Gibson, *Phys. Rev. A* **75**, 063410 (2007).
- [28] M. Fushitani, A. Matsuda, and A. Hishikawa, *Opt. Express* **19**, 9600 (2011).